87/24T

PROBES OF THE QUARK GLUON PLASMA IN HIGH ENERGY COLLISIONS

K. Kajantie

Department of Theoretical Physics and Academy of Finland

Siltavuorenpenger 20 C, 00170 Helsinki, Finland

Larry McLerran

Fermi National Laboratory

P.O. Box 500, Batavia, Illinois, 60510

Shortened title: Probes of Quark-Gluon Plasma

Send proofs to: Larry McLerran; Theory Dept. MS-106; Fermilab; P. O. Box 500; Batavia, Il. 60510

CONTENTS

1 INTRODUCTION

Quark gluon plasma (1) is the high-temperature high-density phase of matter described by the laws of Quantum Chromodynamics. At low temperatures and densities quarks, gluons and color fields are confined to the interiors of strongly interacting particles, hadrons. At high temperatures and densities the hadrons overlap, loose their identity and quarks, gluons and color fields are not confined into hadrons but can move over distances larger than the hadron size, 1 fm.

We expect that the early universe, when it was younger than about 10^{-5} s, was filled with quark gluon plasma (and, at least, photons and leptons). The possible observational consequences, relic cold strange quark matter (2-3), energy density inhomogeneities (4-5), black holes (6), gravitational radiation (2,7), etc., are rather speculative and so far no observational evidence exists. Cold quark gluon plasma or quark matter could also exist in the present universe in the interiors of compact stellar systems; here also no convincing observational evidence exists. For instance, changes in cooling rates have been suggested as such (8). Experiments, on the other hand, on possible quark gluon plasma can be done by studying ultrarelativistic nuclear collisions or very high multiplicity fluctuations in hadron-hadron collisions. What the signals could be, will be studied in this review.

1.1 General Properties of Ultra-relativistic Nucleus-Nucleus Collisions

Even without the prospect of observing quark-gluon plasma, ultra-relativistic nuclear collisions are very interesting and much theoretical work has been devoted to them (9-13). One has mainly tried to predict the rapidity and p_T (or E_T) distributions of produced pions (possibly including neutrals) by extending models developed for hadron-nucleus collisions to nucleus-nucleus collisions: the multi-chain model (10), the additive quark model (11), the dual parton model (12) or the cascade model (13). One also has tried to predict the nuclear stopping power, which describes how baryon number is distributed in the final state (14-16).

Although superficially these predictions have nothing to do with quark-gluon plasmas, they are actually very important for the discussion of any plasma probes. Any thinkable plasma probes have namely a background arising from non-plasma mechanisms and the above model calculations are a method of estimating this background. The model calculations based on particle physics concepts, for instance, are formulated in momentum space while we expect quark-gluon plasma to live in space-time. The experiments thus must find effects which are not naturally described in momentum space, but follow naturally from a glob of matter flowing collectively in space-time and emitting various probes from its interior and surface.

In this context it is important to appreciate that quark-gluon plasma is just the high-temperature high-density phase of QCD matter, in general, and that it would also be very important to observe the low-T low-density phase (hadron gas) and the intermediate mixed phase. An additional complication is that it seems that under present experimental conditions the mixed phase will, on the average, dominate the phenomena. The analysis would be simpler in the pure quark-gluon plasma or the hadron gas phases.

There is now a major experimental effort under way at CERN and BNL to make and study ultra-relativistic nuclear collisions, as well as an effort at FNAL to study the extreme environment provided in high multiplicity fluctuations in $\bar{p}p$ collisions at the Tevatron. The first results from CERN have come at the end of 1986 (17) and more will soon follow.

1.2 Review of Recent Lattice Gauge Theory Results

The only known way of performing first-principle non-perturbative computations on QCD matter is to use lattice Monte-Carlo techniques (18-38). These, however, are only applicable to a rather limited set of static phenomena and there is no first-principle method to compute non-static phenomena. When discussing quark-gluon plasma, it is usually assumed that the plasma behaves like a fluid, i.e., is in local thermal equilibrium (in contrast to a plasma described with the aid of kinetic theory). Thus it is essential to know the equation of state (EOS), which gives the pressure and energy, entropy and net baryon number densities in terms of temperature T and chemical potential μ. This is one important quantity which can be computed with the aid of lattice Monte Carlo, at least for baryon-number free systems, $\mu = 0$.

The fundamentals of finite temperature lattice QCD are reviewed in (37) and more recent developments in (38). We shall here discuss only the question of scaling in the computations, which is a necessary condition for their validity and which was doubtful until recently and the EOS, which is very important for practical purposes. Other notable recent developments are the determinations of static screening lengths for $SU(3)$ (34) and $SU(2)$ (35) and the first attempt to use lattice techniques to determine transport efficients of QCD matter (36).

Finite temperature QCD with only gluons, without quarks, has an order parameter (18-20) which identically vanishes in the confined hadron gas phase and is finite in the gluon plasma phase. On the lattice this is the expectation value $< L(\mathbf{x}) >$ of a trace of a product of $SU(N_c)$ matrices in the time-temperature direction at the spatial site $\mathbf{x}$ (the Wilson-Polyakov loop); the trace arises because of thermal periodic boundary conditions.

A calculation performed on an $N_s^3 \cdot N_t$ lattice corresponds to a system with volume $(aN_s)^3$ and temperature $T = 1/(aN_t)$, where a is the lattice spacing. Of course, the computer accepts only dimensionless numbers, and the distance a is converted to dimensionless numbers by the equation

$$\frac{1}{a} = \Lambda_L (2.3\beta)^{0.42} e^{-1.2\beta} \equiv \Lambda_L f(\beta), \tag{1}$$

where $\beta = 6/g^2$ is the dimensionless number fed into the computer, the expression for $f(\beta)$ follows from perturbation theory and Λ_L is a dimensionful quantity taken from experiment. One thus has

$$\frac{T}{\Lambda_L} = \frac{1}{N_t} f(\beta) \tag{2}$$

and the determination of the critical temperature is done so that one finds at what value of β the order parameter $< L(\mathbf{x}) >$ becomes nonvanishing. This is converted to a physical T by Equation 2. However, the computation is only consistent, if lattices of different N_t give the same physical value of T_c. This is confirmed by the computations in (29-30) and the result is shown in Figure 1. In this the solid curve corresponds to Equation 2 plotted for $T/\Lambda_L = 46.6$

and the points on the curve are from a computation (29) with $N_s^3 = 16^3$ and $N_t = 10, 12, 14$; the non-scaling points are from runs with smaller N_s and $N_t = 2, 4, 6, 8$. From Figure 1 one can see how the opinion on the scaling domain has changed; first one thought that even small lattices with $N_t = 2, 4$ would show scaling (slope parallel to the solid line), but then larger lattices showed evidence for non-scaling. That the scaling only sets in only for $N_t = 10$ is, of course, rather frustrating and implies that very large lattices will be required for detailed results on any phenomena.

Consider then the equation of state for $\mu = 0$, expressed as $\epsilon = \epsilon(T)$. At energy densities low compared to a scale of several hundreds of MeV/fm^3 to several GeV/fm^3 we presumably have a low density gas of the ordinary constituents of hadronic matter, that is, mesons and nucleons. At densities very high compared to this scale, we expect an asymptotically free gas of quarks and gluons. At intermediate energy densities, we expect that the properties of matter will interpolate between these dramatically different phases of matter. There may or may not be true phase changes at these intermediate densities.

The result of a Monte Carlo simulation of the energy density is shown in Figure 2 (26).This is typical of the results of lattice Monte Carlo simulations. The precise values of the energy density are difficult to estimate as is the scale for the temperature. The figure does make clear the essential point, on which all Monte-Carlo simulations agree, that the number of degrees of freedom of QCD matter changes by an order of magnitude in a narrowly defined range of temperature. There is apparently a first order phase transition for SU(3) Yang-Mills theory in the absence of fermions, and a rapid transition which may or may not be a first order transition for SU(3) Yang-Mills theory with two or three flavors of massless quarks.

The results are most accurate for pure gluon matter. Here the computations with lattices as large as 21^3 14 (31) give that the jump in energy density at the phase transition is $\Delta\epsilon = 4.7T_c^4$ with an about 40 % error in the numerical constant (about 10 % error in T_c/Λ_L. To set the scale, note that for free gluon gas $\epsilon = 5.3T^4$. The jump is thus large indeed.

The essential point, the large change in the number of degrees of freedom can be both physically understood and phenomenologically incorporated in terms of a simple bag equation of state. To formulate it, one simply gives the pressures in the quark-gluon plasma phase and the hadron gas phase separately:

$$p_q(T) = g_q\frac{\pi^2}{90}T^4 - B, \tag{3}$$

$$p_h(T) = g_h\frac{\pi^2}{90}T^4, \tag{4}$$

where the effective numbers of degrees of freedom are estimated by assuming that quark-gluon plasma consists of free quarks and gluons (one can also take $N_F = 2.5$ to simulate the effect of the strange quark mass) and hadron gas of free massless pions:

$$g_q = 2\cdot 8 + 2.5\cdot 2\cdot 2\cdot 3\cdot\frac{7}{8} = 42.25,\quad g_h = 3, \tag{5}$$

and B is a bag constant, vacuum energy density, which incorporates the effects of complicated QCD interactions. Including it makes the hadron phase the stable one at low T, i.e., $p_h > p_q$ for $T < T_c$, where the transition temperature T_c is given by

$$B = (g_q - g_h)\frac{\pi^2}{90}T_c^4. \tag{6}$$

Since further

$$\epsilon(T) = Ts(T) - p(T) = Tp'(T) - p(T), \tag{7}$$

it follows from Equations 3-4 that

$$\epsilon_q(T_c)/\epsilon_h(T_c) = 4g_q/g_h - 1/3 \tag{8}$$

so that the large jump in the energy density is simply related to the large change in the number of degrees of freedom. In theories with an arbitrary number of colors, N_c, the jump goes like N_c^2 (since color singlets appear below T_c and gluons dominate above).

2 SPACE-TIME PICTURES OF THE COLLISION

Collision processes in quantum theory are usually simplest to describe in momentum space. This is so since one anyway has to keep the momenta of the initial and final particles fixed. Now one wants to study a glob of matter with a finite extent and finite lifetime. Thus one has to base the arguments of a space-time picture of the collision.

The space-time behavior of quantum electrodynamics was already studied by Landau and Pomeranchuk (39) in 1953. The same was done for the parton picture of strong interactions by Gribov (40) and Bjorken (41), see also (42-46). The picture became particularly relevant when applied to the study of hadron-nucleus collisions (33-34) since in these the nuclear radius provides one with a distance scale to measure space-time behavior with. This has led to the inside-outside cascade model. In nucleus-nucleus collisions a further issue to discuss is thermalisation.

2.1 Inside-Outside Cascade Picture

The physical idea underlying the inside-outside cascade picture is very simple: one assumes that there is a hadronic time-scale τ_0 defined so that partons created in a strong process can only reinteract when their proper time τ is larger than τ_0. One expects that $\tau_0 \sim 1/\Lambda_{QCD} \sim 1 fm/c$ and one has tried to improve this estimate by theoretical means (47-49). Experimentally, however, one has not been able to distinguish between the inside-outside cascade model and various momentum-space models.

The physical consequences of this picture for hadron-nucleus collisions are also simple to see. When the hadron collides with the nucleus, it is immediately, within $1 - 2\ fm$ from the surface, converted to a cloud of inactive partons. Only the partons with $v \cdot \gamma\ \tau_0 < 2R_A$, R_A = target radius, can reinteract within the nucleus and produce a cascade. In other words, partons with rapidity $y > \ln(4R_A/\tau_0) \equiv y_{cr}$ hadronise outside the nucleus. The rapidity distribution dN_π^{pA}/dy of produced pions thus, in this picture, contains an enhancement for $0 < y < y_{cr} \approx \ln 4A^{1/3}$ and behaves like dN_π^{pp}/dy for $y > y_{cr}$.

Comparison with experimental data (48) confirms this highly simplified picture qualitatively but not quantitatively. There is a strong enhancement for small y but also an enhancement relative to pp data at intermediate central region rapidities. This central region enhancement can be understood either in terms of reinteractions of the colliding proton with other target nuclei or in terms of color field effects (48). The highest available energy (200 GeV/c) corresponds to a total rapidity range of $0 < y < 6$ and with $y_{cr} \approx 3$ the separation of the different regions is not yet very clear.

At present the pA data are well understood with momentum space models (multi-chain model, additive quark model, dual parton model, etc.) and there is no need to introduce the space-time inside-outside cascade model. It is also not uniquely clear how the simplest version of this model should be refined. There is thus also no way to fix the value of the essential parameter, τ_0, of this model. A detailed analysis of these issues is carried out in (46). For the study of quark gluon plasma in AB collisions, the inside-outside cascade model nevertheless forms a very convenient starting point.

2.2 Thermalisation

By thermalisation one means the transition of the system to a state in which it consists entirely of bosons and fermions distributed according to the equilibrium distributions

$$n_B(x,p) = \frac{1}{e^{p\cdot u/T} - 1}, \tag{9}$$

$$n_F(x,p) = \frac{1}{e^{(p\cdot u-\mu)/T+1}}, \tag{10}$$

where $T = T(x)$ is the temperature, $\mu = \mu(x)$ the chemical potential (antifermions have the sign of μ inverted) and $u^\mu = u^\mu(x)$ the four-velocity, each depending locally on $x^\mu = (t, x_T, z)$. If the system is locally thermalised, its behavior can be computed from the energy-momentum and baryon number conservation equations $\partial_\mu T^{\mu\nu} = 0$ (equivalent to entropy conservation $\partial_\mu(su^\mu) = 0$) and $\partial_\mu(n_B u^\mu) = 0$ (see Section 3). This clearly is an enormous simplification. Note that the bosonic and fermionic degrees of freedom need not be those corresponding to gluons and quarks, although this is what one expects as a first assumption.

If the system does not thermalise, one may still discuss its behavior in terms of the single particle distribution function $n(x,p)$ and its extensions to several particles, i.e., use kinetic theory. The question of thermalisation and the effects of small deviations from it (dissipation, transport coefficients) have been discussed in (50 - 52) and kinetic theory in (53-56), for reviews, see (57-58). In this context, kinetic theory is also related to the small-x problem in QCD (59).

Consider now a central (zero impact parameter) ultrarelativistic collision of two large nuclei A and B. In case of thermalisation, the sequence of events at zero transverse coordinate and as a function of time t and longitudinal coordinate z could be as shown in Figure 3. Before the collision, for $t < 0$, the partons in the system are distributed in the beam and target according to two (possibly smeared) δ - functions: $n(z,p) \sim \delta(z \pm vt)$. After the collision there follows a pre-equilibrium phase during which individual parton - parton collisions start thermalising the distributions. The entropy of the system increases from the initial value 0.

Figure 3 is drawn assuming that the system thermalises so that the initial temperature is so large that the system initially is in the quark gluon plasma phase. In the inside-outside cascade picture the proper time determines the reinteraction ability of the partons and thus also the initial thermalisation at T_i takes place at a fixed proper time τ_i (60). The further evolution of the system is discussed in Section 3.

Thermalisation here is discussed in an entirely phenomenological way and there exists no quantum theoretic treatment for it. At best one can present qualitative mean free path arguments to motivate it. For instance (47), the mean free path of a quark in QCD matter of energy density ϵ would be

$$\lambda = (5\ ,\ 0.5\ ,\ 0.01) fm \text{ for } \epsilon = (0.15\ ,\ 2\ ,\ 200) GeV/fm^3. \tag{11}$$

Another possibility is to use QCD finite temperature perturbation theory to compute both gluon and quark mean free paths (50-51) with the result

$$\lambda_g = 0.5 - 0.05 fm, \quad \lambda_q = 2 - 0.2 fm \text{ for } \epsilon = 1 - 1000\ GeV/fm^3. \qquad (12)$$

The uncertainties in these estimates are illustrated by the fact that different constant factors T_0 used in the logarithm in $\alpha_s \sim 1/\ln(T/T_0)$ in (50) and (51) gave rise to results differing by almost a factor two for the range of T in question.

Estimates indicate that ϵ of the order of 2 GeV/fm^3 should be attainable even in average collisions of two nuclei. Equations (11-12) indicate that for A more than 100 the transverse size of the system ($\sim R_A$) is clearly larger than the mean free path and there is some motivation for thermalisation. For oxygen (A=16) the situation is very marginal and probably very atypical events with large ϵ would be needed for thermalisation.

One should emphasize that only qualitative arguments can be given for thermalisation and it should basically be regarded as a practical first approximation to be tested experimentally.

2.3 Cascade Simulation of Early Stages

A numerical code simulating the thermalisation process in an ultra - relativistic nucleus - nucleus collision has been developed by Boal (61). The initial momenta of the partons are taken from the standard structure functions of quarks and gluons, and in coordinate space they are randomly distributed within the nucleus so that the density of soft partons is lower than that of hard ones. Partons are then allowed to collide according to the most singular part of the $2 \rightarrow 2$ QCD cross sections. The code can be used, for instance, to follow how the energy density develops.

The limitations of codes of this type are seen from the fact that infrared singularities appear for small x in the structure functions and in the forward direction for the scattering processes and have to be arbitrarily cut off. Physically the reason is that partons are not the only degrees of freedom to describe the process with. Non-perturbative effects also have to be included. This can be done, for example, in the framework of color field models.

2.4 Color Field Models

Color field models (48), (62-67) assume that a color field $\mathcal{E}_l$ is formed between the receding nuclear disks after the collision. Note that the dimension of $\mathcal{E}$ is GeV^2 and that it is related to the total charge Q by $Q = A_T\mathcal{E}_l$, where A_T is the transverse area. Associated with $\mathcal{E}_l$ there is a time scale $\tau_0 = 1/\sqrt{\mathcal{E}_l}$. One thus has at one's disposal a new dimensionful parameter to non-perturbatively model the collision process with.

In this model, there now are three questions to discuss: 1. magnitude of $\mathcal{E}_l$ and its process dependence, 2. conversion of the field to particles, 3. thermalisation of the particles. Beyond that the process is described by fluid hydrodynamics. The color field models thus permit one to describe the entire sequence of events in the nuclear collision process, also the thermalisation stage. There is some support for the model from hadron-nucleus collisions (48) but it both has to be developed further and to be confronted with nuclear collision data to reveal its true potentialities.

3 HYDRODYNAMICS IN ULTRARELATIVISTIC NUCLEAR COLLISIONS

With the possibly large energy densities achievable in ultra-relativistic nuclear collisions, and the large transverse extent of the nuclei, it seems plausible that there is a viable hydrodynamic description of the collisions. Since the transverse extent of the system is large, we expect that at early times, a good approximation is to treat the expansion as entirely longitudinal, that is along the beam axis. The discussion of this expansion is particularly simple in the central region (60), and can be solved for analytically, and will be the subject of Subsection 3.1. The situation in the fragmentation region is a bit more complicated (45,68-71), since the space-time development of the matter is more complicated, and since the distribution of particles in rapidity is not uniform. The study of the fragmentation region is the subject of Section 3.2. At late times in the collision, the expansion becomes 3+1 dimensional. To describe this expansion, 3+1 dimensional hydrodynamic equations must be solved. This is a formidable task, and has been accomplished so far only in the central region (47,72-77). The general outline of the procedure for solving the 3+1 dimensional hydrodynamic equations is the subject of Section 3.3, and the results of these computations are discussed in the sections on experimental probes. At late stages in the collision, the hadrons begin to decouple from one another. At this time the hydrodynamic equations break down. It is at this time that the particle distributions become frozen into their final values. We shall discuss decoupling in Section 3.4.

We continue this introductory discussion with simple arguments that there should be a valid hydrodynamical treatment of the collision by first discussing time scales for expansion, and comparing the expansion time, τ_E, to the collision time τ_C. If the system is to be well approximated as an expanding perfect fluid, that is adiabatically expanding, then $\tau_E >> \tau_C$. In a perfect fluid expansion, the total entropy is conserved. To estimate the time of perfect fluid expansion we can use conservation of entropy. We take the entropy density to be proportional to $N_{dof}T^3$, where N_{dof} are the number of particle degrees of freedom at the time of interest. The volume of the system is proportional to $V \sim t^d$ where t is the time and d is the dimensionality of the expansion. We therefore can relate the initial and final times to the entropy densities as

$$\left(\frac{t_f}{t_i}\right)^d = \frac{N^i_{dof}}{N^f_{dof}} \frac{T_i^3}{T_f^3} \sim 10 - 10^4 \tag{13}$$

At early time, the expansion is one dimensional, and at later times becomes three dimensional. We estimate therefore that $t_f/t_i \sim 10 - 10^3$. Detailed 1+3 dimensional hydrodynamic computations show that the final decoupling time is probably somewhere in the range of $t_f \sim 20 - 50\ fm/c$.

Large nuclei are clearly more favored systems for producing and studying a quark-gluon plasma. This follows simply from the facts that the average energy density achieved is larger, and that the system is physically larger in transverse extent. As discussed in Section 2.1, collision lengths are then likely to be smaller than the size of the system. Experimental information on this has already been obtained at Bevalac energies (see Section 6).

3.1 1+1 Dimensional Results for the Central Region

The hydrodynamic equation in the central region are simplified by the observation that if the rapidity distribution is approximately flat, that is y independent, then the description of this kinematic region should be approximately Lorentz invariant (60). We may introduce the space-time rapidity

$$\eta = \ln\left(\frac{t+z}{t-z}\right) \tag{14}$$

and the proper time

$$\tau = \sqrt{(t^2 - z^2)}. \tag{15}$$

The space-time rapidity equals the momentum space rapidity for freely streaming particles which originated at $x = t = O$. In the hydrodynamic model for the central region, it is also equal to the momentum-space rapidity of the fluid.

The Jacobian of the transformation above transforms $dtdz$ into $\tau d\tau dy$. Since the total entropy is conserved under perfect fluid expansion, we have therefore that the entropy density σ is given by

$$\sigma(\tau) = \sigma(\tau_o) \ \ (\tau_o/\tau) \tag{16}$$

To derive this result, we have used that the entropy density is independent of rapidity. For an ideal gas, we therefore have that

$$T = T_o \ \ (\tau_o/\tau)^{1/3}. \tag{17}$$

The temperature falls very slowly with proper time, and more so at later times. Using a bag model equation of state, one finds that the time to go from an initial temperature temperature of 300 Mev to a temperature of 150 Mev (in the pion phase) is measured in hundreds of Fermis, so long that the effects of transverse expansion must be important.

We may now use this knowledge of the hydrodynamic equations to estimate the initially achieved energy density in terms of the final state conditions. We first note that the hydrodynamic equations are entropy conserving and to a good approximation, multiplicity conserving. The energy density in the initial configuration is given by the number of particles per unit volume times a typical energy per particle, which can be taken as the transverse mass at this time, $m_T^2 = m^2 + p_T^2$. The number of particles per unit volume is simply

$$\frac{N}{V} = \frac{1}{\pi R^2} \frac{dN}{dy} \frac{1}{\tau} \tag{18}$$

In the early stages of the collision when particles are forming, we expect that $m_T \sim 1/\tau$, a situation which is true in a variety of models of particle formation. The initial energy density is therefore

$$\epsilon \sim \frac{1}{\pi R^2} \frac{dN}{dy} m_T^2 \tag{19}$$

In this equation, m_T^2 is measured at the initial time. In general as the system expands, m_T should monotonically decrease, and using experimental values in this equation should provide a lower bound on the energy density at formation.

3.2 1+1 Dimensional Results for the Fragmentation Region

Although the dynamics is more complicated in the fragmentation region, the methods described above may be generalized to include the fragmentation region (69-71). This may be done by providing sources for the hydrodynamic equations corresponding to the materialization of matter after the collision of the two nuclei. The source for the stress energy tensor may be related to the assumed initial distribution of particles. For the baryon number currents, it is possible to treat the baryons as conserved through the entire scattering process (70). The source treatment for the stress energy tensor assumes that the sources correspond to the materialization of particles from pair production, and is consistent with the inside-outside cascade model.

There have been various numerical estimates of the energy and baryon number density in the fragmentation region. Most recent treatments argue that the energy density in the fragmentation region probably approaches that in the central region. At asymptotically high energies, however, we expect that the high multiplicity in the central region will produce asymptotically higher energy densities.

The achieved baryon number densities are quite controversial. The latest estimate shows that the baryon number density may become up to ten times greater than that of nuclear matter (70), in sharp contrast with older results (69) where values only twice nuclear matter were found. The new result is in accord with ancient order of magnitude estimates (45).

3.3 1+3 Dimensional Results

To handle the late stages of the matter evolution, when the expansion becomes three dimensional, 1+3 dimensional hydrodynamic equations must be solved. This is not too complicated in the central region. In the central region, Lorentz invariance eliminates the rapidity as a variable. If we assume central collisions, there is azimuthal symmetry. The resulting hydrodynamic equation is effectively a 1+1 dimensional problem.

The solution of the three dimensional expansion of the system is important for computing transverse momentum and energy distributions. Such a computation can relate enhancements in these distributions to properties of the equation of state, which in fact determines the solution to the hydrodynamic equations. Such a solution also allows for detailed computations of the spectra of photons and dileptons, as well as strange particle production, as will be discussed in later sections.

For ideal gas equations of state, this problem is easily solved by the method of characteristics (72-73). For a bag model equation of state, the method of characteristics is no longer applicable, since a shock front develops in the transverse rarefraction at the interface of the mixed phase with the hadron gas phase (74-75). A variety of methods have been used to deal with this mathematical problem (74-76). The entire time evolution of the system from very high temperature to asymptotically low temperatures can now be solved for in a minimum of computer time.

The treatment of the hadronization of the plasma via a mixed phase is subject to some criticism in these approaches. If there is truly a first order transition between plasma and a hadron gas, such an approach may be invalidated by supercooling of the plasma, and various deflagration and detonation singularities may develop (78-81). If the transition is weak first order or second order, the treatment of the transition region as a mixed phase is probably quantitatively good.

There are a variety of uncertainties in these computations concerning the initial conditions. Only one unknown parameter, the multiplicity can be determined from experiment. The initial temperature effects the computation of dilepton distributions, and therefore the measurement of the dileptons may give a measure of this. Uncertainties in the shape of the initial matter distribution are not so important.

The treatment of decoupling follows the classical analysis of Cooper and Fry (82). It is assumed that at some fixed temperature, the hadrons decouple instantaneously from one another, and become free streaming non-interacting particles. Such an idealization leaves out much physics, such as entropy production at decoupling. If decoupling happens at an energy density much lower than that of the hadron gas at the phase transition temperature, then we expect that this sloppy treatment should provide a good approximation

3.4 Decoupling and Pion Cascade in Late Stages

To properly handle the problem of decoupling, and to test the assumptions underlying the hydrodynamic computations, a cascade simulation of the hadronic gas phase is useful. If the hadron gas is cool enough, then the hadron gas is well approximated as a pion gas. The scattering of pions may be estimated from low energy phase shift analysis.

Such a pion cascade is being developed by Bertsch et. al. (83). In addition to being able to better treat decoupling and to better understand the quality of the hydrodynamic approximation, the spectrum of low energy photons and dileptons might be computed. In the low energy region, these photons and dileptons are emitted by the bremstrahlung process. Their distribution reflects the space-time history of the system at late times as the hadron gas freezes out.

4 PROBES IN GENERAL

QCD matter formed in ultra-relativistic nucleus-nucleus collisions is at most a few tens of fm across and lives at most a few tens of fm/c. It is thus clear that no direct probes are feasible and that all diagnostics must be indirect and based on measuring the decay products of the matter. The general strategy of observing QCD matter and, in particular, its quark gluon plasma phase could thus be as follows:

1. Measure everything possible: differential distributions of all types of particles and cross correlate these with each other. Check if there is anything which cannot be understood in terms of the various models for particle production making no reference to space-time. To have evidence for matter in local thermal equilibrium there must be something which needs space-time for its explanation.

2. Find evidence for collective flow irrespective of the phase the matter is in.

3. Find evidence for matter in the quark gluon plasma phase, in particular.

4. If quark gluon plasma is found, diagnose also its properties. How does it hadronise? What are the kinetic properties of the phase transition?

The following list of experimental probes (with the physics they are sensitive to) can be presented:

1. Dileptons (quark gluon plasma, T_i (for $1 < M < 3GeV$), T_{PT}, collective flow (for $M \approx 1GeV$), plasma expansion, impact parameter, resonance melting, low mass pairs and space-time evolution),

2. Photons (as dileptons but for M dependent effects),

3. Jets (scattering cross section of quarks and gluons with plasma and hadron gas),

4. ϕ and ψ production (quark gluon plasma),

5. Hadron p_T distributions (equation of state, collective flow),

6. Strangeness (existence of hadron gas, dynamics of expansion),

7. Pion correlations (size and lifetime of the system).

All these probes should be measured together with the associated pion multiplicity dN_π^{AB}/dy or the total transverse energy E_T with the understanding that the larger these are, the more likely it is that the system will initially be in the quark gluon plasma phase. There should also be a separate trigger on small impact parameter collisions, like a cut in nuclear fragmentation or forward energy flow. The analysis of correlated variables will be complicated and one cannot argue that any of the probes will yield an unambiguous signal for the plasma. Using several different probes it should, however, be possible to make a convincing case.

The size of the smaller one of the colliding nuclei is also a very important parameter. The first experiments at ultra-relativistic energies will be done with rather small nuclei, like oxygen, in the beam. It is quite likely that these will not yet reveal unambiguous matter effects. With the experience from Bevalac energies one might expect that A at least 100 will be needed before collective effects can be observed.

The various probes can also be characterized as volume or surface probes. In the former case we have a probe (photon, dilepton, ϕ, ψ, jet) which is formed in the inside of the plasma and leaks out of it giving information of the conditions inside. In the latter case the probe is either formed at the surface (hadron p_T, strange particles) or relates to the system as a whole (interference effects). Volume probes are clearly more direct.

5 THE CORRELATION OF p_T AND $\frac{dN}{dy}$

The correlation between p_T and dN/dy reflects properties of the equation of state of matter (84,85). A measurement of such a correlation is in principle straightforward.

5.1 A Spherically Symmetric Example

A correlation between p_T and dN/dy is easily seen from the example of a spherically expanding gas. We assume that at some initial time, there is a spherically symmetric drop of hadronic matter of uniform density matter at rest. We then allow the system to hydrodynamically expand. We assume we know the volume of the initial system, V_o. We measure the total energy of all particles and the total multiplicity of particles in the final state. Since the system is slowly expanding at late times, the entropy of particles in the final state is known assuming the particles were produced thermally from a weakly interacting gas. Since energy and entropy are conserved in the expansion of a perfect fluid, the energy and entropy of the final state is that of the initial state. We can therefore experimentally measure the correlation between say p_T, which is proportional to E/S, and the energy density (86,87). We can compare this to a theoretically predicted correlation determined by knowing the equation of state.

A plot of E/S versus ϵ is shown in Figure 4. for a bag model equation of state. The generic features of this curve are straightforward to understand. At low temperature, in the pion gas phase, and high temperatures, in the plasma phase, $E/S \sim T$. The energy density in these two phases goes as $\epsilon \sim N_{dof}T^4$. Since the number of degrees of freedom changes at the transition, there is a gap between these two curves. The gap is filled by the region where the plasma cools into a pion gas. This happens at a fixed T, and almost fixed E/S, for varying ϵ.

5.2 Numerical Results for Head-On Collisions of Equal A Nuclei

There are several problems when arguments like the above are applied to the more realistic expansion scenarios appropriate for central collisions of heavy nuclei. First p_T is not conserved since longitudinal expansion causes the transverse momentum of individual particles to be converted into un-observed collective flow in the longitudinal direction. A correlation between p_T and say multiplicity is therefore weaker than is the case for spherical expansion. It also depends more on the detailed numerical simulation of the hydrodynamic equations. Also, the initial conditions for the matter are not so well known. The final state decoupling and perhaps a phase change may produce some entropy. Fortunately these problems do not appear to generate much dispersion in the numerical results for such a correlation (74). Finally, a severe limitation of present hydrodynamic simulations is that they are limited to the central region of impact parameter zero collisions. If we only have a multiplicity trigger to measure the degree to which collisions occurred at zero impact parameter, then the low multiplicity events will always be dominated by large impact parameter, and their contributions have not been computed. The present computations may therefore only provide information on head-on collisions and their fluctuations. Since the number of particles is already large, the fractional fluctuations in the multiplicity for such head-on collisions is small.

There is also the potential problem of backgrounds from conventional processes such as mini-jets obscuring the p_T enhancement from a quark-gluon plasma (89). At energies typical of the SPS collider, production of mini-jets is presumably responsible for the high multiplicity events. In nuclear collisions at energies less than or equal to those proposed at RHIC, mini-jets are not expected to be a large background since the beam energy is low. Moreover, mini-jets should thermalize in the high multiplicity environment typical of central collisions of large nuclei, thus changing the initial conditions by making the matter initially a little hotter, but yielding a correlation between p_T and dN/dy which may be computed by hydrodynamics.

In Figure 5, the results of a hydrodynamic computation of p_T vs dN/dy is shown for an equation of state typical of the bag model and a pion gas equation of state. The difference between these curves is large suggesting that an experimental probe of this correlation can resolve various equations of state. A general feature is that the softer is the equation of state, the softer is the p_T. A quark-gluon plasma produces lower p_T particles at fixed multiplicity than does a pion gas.

In Figure 6, the same correlation is shown for head-on collisions of various nuclei. The curves approximately scale as a function of $1/A \quad dN/dy$. The factor of $1/A^{2/3}\ dN/dy$ arises because the result must be proportional to the multiplicity per unit area. An additional suppression by a factor of $A^{1/3}$ arises due to the softening effects of longitudinal expansion.

As has been argued by Shuryak (84), heavy particles should show the effect of collective transverse expansion more strongly than do light particles. This is shown in Figure 7, where p_T is computed for pions, kaons and nucleons as a function of multiplicity. The physical origin of this effect is that in fluid expansion, there is a collective fluid velocity v. Heavier particles have larger masses and therefore $p = mv\gamma$ is correspondingly larger.

In Figure 8, the p_T distributions of pions, kaons and nucleons are shown. The distribution of nucleons clearly shows the effects of collective flow with the local maximum in dN/d^2p_T at $p_T \sim 1$ Gev.

In Figure 9, an attempt is made to fit the experimentally observed correlation between p_T and transverse energy per unit rapidity as seen in the JACEE collaboration (88). The JACEE data rises too rapidly to be explained by a quark-gluon plasma. The data does seem to be fit by a pion gas model (dashed line), but the temperatures where the system would be required to be in an ideal pion gas are quite large, and we consider this explanation unlikely. Either there is some non-thermal source of high p_T particles in the JACEE data, something is wrong with the space-time picture of the collisions (86), or something is wrong with the data analysis.

6 FLUID EFFECTS AND JETS

One of the most important phenomena to confirm is that the matter produced in nuclear collisions behaves collectively as a fluid and many of the probes discussed here (p_T effects, dileptons) give information on this. This question has already been studied experimentally at Bevalac energies (90-91). The data obtained also throws some light on the size of systems necessary for fluid dynamic effects to become important.

In collisions of nuclei of small impact parameter, single particle collisions occur at large transverse momentum. The nuclei do not collectively flow in a given transverse direction unless there are subsequent rescatterings among the constituents of the nuclei. If these subsequent rescatterings do not occur, the transverse momentum of each particle is randomly oriented. To get collective flow, one needs rescattering, and this should be enhanced in collisions at small impact parameter, and collisions of large A nuclei.

In Figure 10, the flow angle is plotted for various measures of the impact parameter (large impact parameters at the top and small at the bottom of the figure) for various nuclei (small on the left and large on the right). Little evidence of flow is shown for nuclei as large as calcium, and collective effects begin to become important for nuclei of the size of niobium.

Another potential experimental probe of quark gluon plasma is the quenching of jets. The rescattering of jets after their production in a quark-gluon plasma in principle provides a probe of the plasma and hadronic matter as the jet plows through the evolving system (92-94). The jets will scatter from the constituents of the plasma as well as the constituents of hadronic matter which forms later. The degree of scattering is a measure of the quark-matter or gluon-matter cross section.

This scattering can dramatically change quantities such as the jet acoplanarity, and can produce phenomena such as single jets. Theoretical predictions of jet acoplanarity for a variety of jet p_T on a variety of nuclei have been performed (94). For nuclei with $A \sim 100$, and for jets of mass 10 Gev, the differences induced by the presence of a matter distribution are striking, and the rescattering removes the planar nature of the jets. Even at jet mass of 20 GeV, the difference is still significant, and the jets are remarkably acoplanar. In fact at these masses, the jets are probably largely extinguished.

The experimental measurement of this acoplanarity is very difficult. Particles with low rapidities along the jet axis, $y < 2$, must be somehow removed from the sample of particles contributing to the acoplanarity distribution. These low p_T particles arise from conventional low p_T processes, and have little in common with the high p_T particles associated with the jet.

7 DILEPTONS

7.1 General Properties; Correlation Between Mass and Time of Emission

Dileptons from the plasma (95-106) are dominantly formed by the process $q + \overline{q} \rightarrow \gamma^* \rightarrow l^+ + l^-$ and from the hadron gas by $h + \overline{h} \rightarrow l^+ + l^-$; for small dilepton mass M also bremstrahlung is important. The rate per unit time and volume is easy to estimate and depends only on the temperature T (and dilepton variables). In the hydrodynamical scenario (Section 3) the space-time history of the system is known and the predicted dilepton rate in nuclear collisions can be computed. Ideally one compares this prediction with the experimentally observed rate; agreement would verify the scenario and determine its parameters.

The general strategy of using dileptons as probes of quark-gluon plasma is as follows. Measure the process $A + B \rightarrow l^+ + l^- + X$ as differentially as possible using as variables the mass M, rapidity y, p_T of the dilepton, forward energy flow (as impact parameter trigger), associated hadron multiplicity dN_h^{AB}/dy, transverse energy E_T of the event, etc. What is expected can be conveniently discussed in terms of M:

1. At large M ($M > 3GeV$, preferably $M > 10GeV$) one observes the entirely non-thermal single collision Drell-Yan mechanism. The measured rate determines the structure functions of quarks in nuclei. There is no correlation between the pion and dilepton rates. The Drell-Yan pairs are emitted at times $t < 1/M < 0.1\ fm$.

2. For $1 < M < 3\ GeV$ (the limits are very rough) and for events having large dN_π/dy the dilepton rate is proportional to the square of dN_π/dy and diagnoses the properties of quark gluon plasma. These pairs are also emitted very early in the course of the expansion (one has dominantly $M \sim 5T$ and T_i is of the order of a few hundred MeV for times of the order of a few fm). Hardly any transverse flow has time to develop. The rapidity fluctuations of pions and dilepton are correlated.

3. For $M \sim 1\ GeV$ the pairs are emitted from the matter after it has cooled down to the transition temperature T_{PT} or even below it to the hadron gas phase. The times involved may be of the order of tens of fm. Transverse flow will have time to develop.

The mass-time correlation is a potentially very useful property of the dilepton signal since it permits one to follow the time development of the system. In practice, it may be very difficult to unravel this signal in a clean form. In the interesting mass range between 1 and 3 GeV there are namely several backgrounds from bremstrahlung, decays of charmed particles, pre-equilibrium emission, etc.

7.2 Use of Dileptons to Diagnose Quark Gluon Plasma

How dileptons of masses around 2 GeV diagnose properties of quark gluon plasma is illustrated by Figure 11. The figure is computed (100) for two different 1+3 dimensional flows in central U+U collisions having the same total entropy (same $dN_\pi/dy = 26 \cdot 238$) but different initial temperatures and initial times, $T_i = 350$ MeV, $\tau_i = 1.5$ fm and $T_i = 500$ MeV and $\tau_i = 0.5$ fm; the transition temperature is assumed to be 200 MeV. The curve marked Mixed Phase gives the yield of dileptons from this fixed $T = 200$ MeV; it is independent of T_i and decreases fast above $M = 1$ GeV. The quark phase contribution, on the other hand, depends on T_i so that the larger T_i, the larger the rate for large masses. For this very large multiplicity, the Drell-Yan rate is clearly below the thermal rate.

Figure 11 also illustrates the complexity inherent in plasma diagnostics. When the data is plotted for various dN_π/dy, only the combination $T_i^3\tau_i$ is fixed. For each value of dN_π/dy still different values of T_i are possible. It is thus not possible to determine the value of T_i for each event separately; only the average value of T_i for the events having a given value of dN_π/dy.

A further reservation is that pre-equilibrium emission is not yet included. It could affect the high-M end of Figure 11.

7.3 Use of Dileptons to Diagnose Collective Flow

Earlier we have seen how the dependence of $< p_T >$ on mass can be an indication of collective flow (which has to be transverse to be observable). A qualitatively similar mechanism operates for dileptons: if they are emitted from a matter flowing transversally, an increase in their transverse momentum is observed. The transverse flow has time to develop only if the system lives longer than $R_A/v_s \approx 10$ fm (as is confirmed by $1+3$ dimensional numerical computations). By then the system has cooled to temperatures ~ 200 MeV and pairs with $M \sim 1$ GeV are dominantly emitted. Transverse flow effects can thus be searched for by looking at pairs with $M \approx m_\rho$.

A concrete example is shown in Figure 12. Here the dilepton rate for $M = 0.8$ GeV and $y \approx 0$ is shown as a function of the transverse mass $M_T = \sqrt{p_T^2 + M^2}$, separately for the mixed phase ($T = 200$ MeV) and the quark gluon plasma phase for both no transverse flow (1 + 1 dimension hydro) and with transverse flow (1 + 3 dimensional hydro). The flow parameters are as indicated in the Figure. The quark gluon plasma phase has no time to develop transverse flow and is virtually unaffected by it. The mixed phase lives very long and ultimately develops a rapid transverse flow. The effect on the predicted rate is strong; the rate for $p_T =$ a few GeV is changed by orders of magnitude.

The same effect can be seen in some more detail by plotting the dilepton rate as a function of M for $M_T =$ 1,2,3,4 GeV, say (105). If there is no transverse flow, the ρ peak is clearly seen for small M_T but at large M_T the M independent quark gluon plasma phase dominates and the ρ peak disappears (dashed line in Figure 12). When transverse flow is included, the ρ peak persists until large M_T. This is thus the range to study to observe collective flow with dileptons.

7.4 Resonance Melting, ψ Production

The vector meson resonances $(\rho, \omega, \phi, \psi)$ are easy to observe in the dilepton spectrum. On the other hand, they clearly cannot exist in the quark gluon plasma phase, they melt away if hadron gas is heated above the transition temperature (103). Naively one thus could expect their absence to be a signal for the plasma phase. However, they certainly are formed during the mixed and hadron phases (and couple to virtual photons which leak out of the system) and the problem becomes a quantitative one.

The situation with the ρ and ω resonances was discussed above: they are abundantly formed during late stages of the process and the melting signal becomes a signal for collective flow. With the ψ (and to a lesser extent, the ϕ) the situation is possibly different (106). The expected dominant production mechanism is two-gluon fusion $gg \rightarrow \bar{c}c \rightarrow \psi$. This would take place very early, before or during the plasma stage but would then actually be hindered by the existence of the plasma. The magnitude of the ψ peak above the dilepton background could thus be decreased if plasma existed. This is a very straightforward experimental quantity to study, but one must remember that the prediction of cross sections of processes involving charmed quarks has been notoriously difficult. In this case additional processes and surface effects could also give a sizable contribution.

8 STRANGENESS

Strange particles seen in the detectors of a nuclear collision experiment are all formed at decoupling of the system - provided that an expanding system of matter at all is seen. They thus have no direct contact with a possible quark gluon plasma phase existing early during the history of the system and, if at all, they are a very indirect probe of the plasma phase. On the other hand, if one could experimentally prove that the strange particles decouple from a hadron gas in local thermal equilibrium, they could serve as a signal for the existence of this system and as a probe of its properties. This in itself makes it worth to carefully study the production of strange particles.

There has been much work done on the subject of strange particle production in heavy ion collisions (107-116). It was originally believed that in a quark-gluon plasma in thermal equilibrium, there would be a larger strangeness abundance than in a corresponding hadron gas, and it was successfully argued that in a quark-gluon plasma as produced in a heavy ion collision, there would be time to produce an equilibrium abundance of strange quarks (107,108). The first argument has been disputed (109- 115), while the second argument has been supported by various computations.

While a hadron gas may be almost as rich in strange hadrons as is a quark-gluon plasma, if the temperature at which strangeness production decouples is sufficiently large, then there is quite likely a large strangeness abundance. We can see that this is the case by computing the strangeness abundance under the conservative assumption of a hadron gas. The result is quite sensitive to the assumed decoupling temperature for strangeness, but this is precisely why a measurement of this quantity is interesting.

Consider first strange mesons in the central region. In pp collisions the K/π ratios are of the order of 0.1. For example, in 270 GeV + 270 GeV $p\bar{p}$ collisions the average number of $\pi^+ + \pi^-$ is 24 and that of $K^+ + K^-$ is 2.2. In thermal equilibrium the density of a boson with mass m and degeneracy factor g would be (K_2 is a Bessel function)

$$n = \frac{g}{2\pi^2}Tm^2[K_2(\frac{m}{T}) + \frac{1}{2}K_2(\frac{2m}{T}) + \ldots]. \tag{20}$$

Evaluating this at T = 200, 160, 100 MeV gives $(\pi^+ + \pi^-)/(K^- + \overline{K}^0) \approx 0.4$, 0.3, 0.1. Observing an enhanced K/π ratio would thus be a signal for the kaons coming from hadron gas in thermal equilibrium and the magnitude of the ratio could be a probe of the decoupling temperature. Note that the mass dependence of p_T discussed in Section 5.2 tests the same fact but also the collective flow of the system.

With the above numbers there is the risk that, although the hadron gas system exists, the decoupling temperature is so close to 100 MeV that the K/π ratio is so close to its value 0.1 in non-thermal pp collisions that no firm conclusions can be made. This enhances the importance of performing in proper kinetic theory analysis of decoupling from the hadron gas.

One can also try to extend the above arguments to baryons in the central region. Again, at the $p\bar{p}$ collider the average numbers of $p+\bar{p}, n+\bar{n}, \Lambda + \Sigma^0 +$ antiparticles, $\Sigma^+ + \Sigma^- +$ antiparticles, $all \Xi's$ are 1.45, 1.45, 0.53, 0.27, 0.2, respectively. The leading baryon/antibaryon, one of each per event, were excluded here. In other words, for produced baryons, strange/nonstrange $= 1.0/2.9 \approx 0.3$. In thermal equilibrium a computation similar to the above gives strange/nonstrange = 0.7, 0.5, 0.3 at $T = 200, 150, 100$ MeV. Again the value 0.3 observed in non-thermal pp collisions is obtained at T = 100 MeV and higher values of the decoupling temperature may lead to enhanced strangeness. Due to the low baryon density, a proper kinetic theory computation would be even more important for them than for mesons.

For baryons in the fragmentation regions the situation is still more complicated. This case is treated, for instance, in (116).

In summary, it is very hard to connect the strange particles observed with possible quark-gluon plasma in a reliable way. On the other hand, it is very important to study their production experimentally, to see if anything unexpected takes place.

9 HANBURY-BROWN-TWISS

The Hanbury-Brown-Twiss effect arises from the interference of the matter waves of identical particles as they are measured in coincidence experiments. This effect arises since there are two possible paths of particles from emission to two coincidence detectors. If the amplitudes for this process are summed and squared, even for incoherent emission amplitudes, the result depends on the distance of separation of the emission regions. For relative particle momentum $k \leq R$, the detection probability is modified from its incoherent form.

The measurement of identical particles closely correlated in momentum therefore allows the possibility of measuring properties of the space-time evolution of matter produced in heavy ion collisions (117-119). One can in principle measure the size and shape of the matter at the temperature when decoupling occurs, and perhaps verify the existence of an inside-outside cascade description.

The theoretical predictions of the Hanbury-Brown-Twiss correlation are complicated by a variety of factors. The interference may be obscured by final state hadronic interactions which are difficult to compute. The space-time profile of decoupling is not yet so well known, and depends on details of the hydrodynamic simulations as well as the details of decoupling. Assuming that decoupling occurs at late times and large transverse sizes, t, $r_T \leq R$, the correlation occurs only for very small relative momentum, and is very difficult to measure.

References

[1] Collins, J. C., Perry, M., *Phys. Rev. Lett.* 34:1353(1975)

[2] Witten, E.,*Phys. Rev. D*30:272(1984)

[3] Freedman, B. A., McLerran, L., *Phys. Rev. D*17:1109(1978)

[4] Applegate, J. H., Hogan C. J., *Phys. Rev. D*31:3037(1985)

[5] Kajantie, K., Kurki-Suonio, H., *Phys. Rev. D*34:1719(1986)

[6] Hogan, C. J., *Phys. Lett.* 113B:172(1983)

[7] Hogan, C. J., *Mon. Not. R. Astr. Soc.* 218:629(1986)

[8] Iwamoto, N., *Phys. Rev. D*28:2353(1983)

[9] Bialas, Andrzej, in Jacob, M., Satz, H., ed. *Quark matter formation and heavy ion collisions*; Proc. of the Bielefeld Workshop May 1982. Singapore: World Scientific (1982)

[10] Kinoshita, K., Minaka, A., Sumiyoshi, H., *Z. Phys. C* 8:205(1981)

[11] Bialas, A., Czyż, W., Lesniak, L., *Phys. Rev. D*25::2328(1982)

[12] Capella, A., Pajares, C., Ramallo, A. V., *Nucl. Phys. B*241:75(1984)

[13] Otterlund, I., Garpman, S., Lund, I., Stenlund, E., *Z. Phys. C*20:281(1983)

[14] Busza, W., Goldhaber, A. S., *Phys. Lett.* 139B:235(1984)

[15] Hüfner, J., Klar, A., *Phys. Lett.* 145B:167(1984)

[16] Daté, S., Gyulassy, M., Sumiyoshi, H., *Phys. Rev. D*32:619(1985)

[17] Bamberger, A., et al., CERN Preprint CERN/EP 86-194(1986)

[18] Polyakov, A., M., *Phys. Lett.* 72B:427(1978)

[19] Susskind, L., *Phys. Rev.* *D*20:2610(1979)

[20] L. McLerran and B. Svetitsky, *Phys. Lett.* 98B:195 (1981), *Phys. Rev.* *D*24:450 (1981).

[21] J. Kuti, J. Polonyi, and K. Szlachanyi, *Phys. Lett.* 98B:199 (1981).

[22] K. Kajantie, C. Montonen and E. Pietarinen, *Zeit. Phys.* C9:253 (1981).

[23] J. Engels, F. Karsch, I. Montvay and H. Satz, *Phys. Lett.* 101B:89 (1981); *Nuc. Phys.* B205:545 (1982).

[24] T. Celik, J. Engels, and H. Satz, *Phys. Lett.* 125B:411 (1983); *Phys. Lett.* 129B:323 (1983).

[25] T. Celik, J. Engels and H. Satz, *Phys. Lett.* 133B:427 (1983); *Nuc. Phys.* B256:670 (1985).

[26] R. Gavai and F. Karsch, *Nuc. Phys.* B261:273 (1985).

[27] Fukugita, M., Ukawa, A., *Phys. Rev. Lett.* 57:503(1986)

[28] A. Kennedy, B. J. Pendleton, J. Kuti and K. S. Meyer, *Phys. Lett.* 155B:414 (1985).

[29] Gottlieb, S. A., Kuti, J., Toussaint, D., Kennedy, A. D., Meyer, S., Pendleton, B. J., Sugar, R. L., *Phys. Rev. Lett.* 55:1958(1985)

[30] N. Christ and A. Terrano, *Phys. Rev. Lett.* 56:111 (1986).

[31] Gottlieb, S. A., Kennedy, A. D., Kuti, J., Toussaint, D., Meyer, S., et al., *The latent heat of pure gluon deconfinement*, (1987)

[32] Redlich, K., Satz, H., Bielefeld preprint BI-TP 85/33(1985)

[33] DeGrand, T. A., DeTar, C. E., Colorado preprint COLO-HEP-131(1986)

[34] DeGrand, T. A., DeTar, C. E., *Phys. Rev. D*34:2469(1986)

[35] Kanaya, K., Satz, H., Bielefeld preprint BI-TP 86/16(1986)

[36] Karsch, F., Wyld, H. W., Urbana preprint ILL-(TH)-86-51(1986)

[37] Satz, H., *Ann. Rev. Nucl. Part. Sci.* 35:245(1985)

[38] Svetitsky, B., *Proc. of Quark Matter '86, Nucl. Phys. A*, to be published

[39] Landau, L., Pomeranchuk, I., *Dokl. Akad. Nauk SSSR* 92:535(1953) and 92:735(1953). In *Collected papers of Landau*, ed. D. ter Haar, papers 75 and 76,. New York: Gordon and Breach, 1967

[40] Gribov, V. N. 1973. *Space-time description of hadron interaction at high energies*. VIII Leningrad nuclear physics winter school.

[41] Bjorken, J., *Lectures at the DESY Summer Institute*, (1975). Proceedings edited by J. G. Korner, G. Kramer, and D. Schildnecht (Springer, Berlin, 1976).

[42] Casher, A., Kogut, J., Susskind, L., *Phys. Rev. D*10:732(1973)

[43] Kancheli, O. V., *Pisma Zh. Eksp. Teor. Fiz.* 18:469(1973)

[44] Levin, E. M., Ryskin, M. G., *Yad. Fiz.* 31:429(1980)

[45] R. Anishetty, P. Koehler and L. McLerran, *Phys. Rev. D*22:2793 (1980); L. McLerran, *Proc. of 5th High Energy Heavy Ion Study*, Berkeley, Ca. (1981).

[46] Kisiliewska, D. K., *Acta Physica Polonica B*15:1111(1984)

[47] H. von Gersdorff, L. McLerran, M. Kataja, and P. V. Ruuskanen, *Phys. Rev. D*34:794 (1986).

[48] A. Kerman, T. Matsui, and B. Svetitsky, *Phys. Rev. Lett.* 56:219 (1986).

[49] Hwa, R., Kajantie, K., *Phys. Rev. Lett.* 56:696(1986)

[50] Hosoya, A., Kajantie, K., *Nucl. Phys. B*250:666(1985)

[51] Danielewicz, P., Gyulassy, M., *Phys. Rev. D*31:53(1985)

[52] Gavin, S., *Nucl. Phys. A 435:826(1985)*

[53] Heinz, U., Phys. Rev. Lett. 51:351(1983); Phys. Lett. 144B:228(1984); Ann. Phys. 161:48(1985); Phys. Rev. Lett. 56:93(1986)

[54] Elze, H.-Th., Gyulassy, M., Vasak, D., Nucl. Phys. B276:706(1986); Phys. Lett. 177B:402(1986)

[55] Bialas, A., Czyż, W., Phys. Rev. D30:2371(1984); Z. Phys. C 28:255(1985); Acta Physica Polonica B 17:635(1986)

[56] Heinz, U., Ann. Phys. 168:148(1986)

[57] Matsui, T., Proc. of Quark Matter '86, Nucl. Phys. A, to be published

[58] Heinz, U., Proc. of Quark Matter '86, Nucl. Phys. A, to be published

[59] Gribov, L. V., Levin E. M., Ryskin, M. G., Physics Reports 100:1(1983)

[60] J. Bjorken, Phys. Rev. D27:140 (1983).

[61] Boal, D. H., Phys. Rev. C, to be published

[62] Ehtamo, H., Lindfors, J., McLerran, L., Z. Phys. C 18:341(1983)

[63] Biro, T. S., Nielsen, H. B., Knoll, J., Nucl. Phys. B245:449(1984)

[64] Bialas, A., Czyż, W., Nucl. Phys. B267:242(1986)

[65] Kajantie, K., Matsui, T., Phys. Lett. 164B:373(1985)

[66] Gyulassy, M., Iwazaki, A., Phys. Lett. 165B:157(1985)

[67] Gatoof, G., Kerman, A. K., Matsui, T., The flux-tube model for ultra-relativistic heavy ion collisions, MIT preprint CPT 1338(1986)

[68] K. Kajantie and L. McLerran, Phys. Lett. 119B:203 (1982); Nucl. Phys. B214:261 (1983).

[69] K. Kajantie, R. Raitio and P. V. Ruuskanen, Nucl. Phys. B222:152 (1983).

[70] L. Csernai and M. Gyulassy Nucl. Phys. A, to be published

[71] Chu, M.-C., Phys. Rev. D34:2764(1986)

[72] G. Baym, B. Friman, J.-P. Blaizot, M. Soyeur and W. Czyz, Nucl. Phys. A407:541 (1983)

[73] A. Bialas and W. Czyz, Acta. Phys. Pol. B15:229 (1984).

[74] Kataja, M., Ruuskanen, P. V., McLerran, L. D., von Gersdorff, E., Phys. Rev. D34:2755(1986)

[75] Friman, B., Kajantie K., Ruuskanen, P. V., Nucl. Phys. B266:468(1986)

[76] J. P. Blaizot and J. Y. Ollitrault, Saclay Preprint (1986).

[77] O. D. Chernavskaya and D. C. Chernavskaya, Kiev Preprint ITP-86-66 (1986).

[78] Van Hove, L., Z. Phys. C21:93(1983); 27:135(1985)

[79] Friman, B. L., Baym, G., Blaizot, J.-P., Phys. Lett. 132B:291(1983)

[80] Gyulassy, M., Kajantie, K., Kurki-Suonio, H., McLerran, L., Nucl. Phys. B237:477(1984)

[81] Danielewicz, P., Ruuskanen, P. V., Phys. Rev. D35:344(1987)

[82] Cooper, F., Fry, G., Phys. Rev. D10:186(1974)

[83] G. Bertsch, L. McLerran, P. V. Ruuskanen, and E. Saarkinen (in preparation).

[84] E. V. Shuryak and O. Zhirov, Phys. Lett. 89B:253 (1979); Yadern. Fiz. 21:861 (1975).

[85] L. van Hove, Phys. Lett. 118B:138 (1982).

[86] H. von Gersdorff, J. Kapusta, L. McLerran and S. Pratt, Phys. Lett. 163B:253 (1985).

[87] K. Redlich and H. Satz, Phys. Rev. D33:3747 (1986).

[88] T. Burnett at. al., Phys. Rev. Lett. 50:2062 (1983).

[89] Halzen, F., Gaisser, T. K., Phys. Rev. Lett. 54:54(1985); Jacob, M., Landshoff, P. V., CERN Preprint CERN-TH.4562/86, 1986

[90] G. Buchwald, G. Graebner, J. Theis, S. Maruhn, W. Greiner and H. Stöcker, Phys. Rev. Lett. 52:1594(1984); Nucl. Phys. A 418:625(1984)

[91] H. A. Gustafsson et. al. Phys. Rev. Lett. 52:1590(1984)

[92] J. D. Bjorken, FNAL Preprint, Fermilab-Pub-82159-T (1982).

[93] D. Appel, Phys. Rev. D33:717(1986).

[94] Blaizot, J. P., McLerran, L., Phys. Rev. D34:2739(1986)

[95] Feinberg, E., L., Nuovo. Cim. 34A:391(1976)

[96] Shuryak E., V., Zhirov, O., Yadern. Fiz. 24:195(1976); Shuryak, E., V., Phys. Lett. 78B:150(1978); Shuryak, E. V., Sov. J. Nuc. Phys. 28:408(1978)

[97] McLerran L., Toimela, T., Phys. Rev. D31:545(1985)

[98] Hwa R., Kajantie, K., Phys. Rev. D32:1109(1985)

[99] Kajantie, K., Kapusta, J., McLerran, L., Mekjian, A., Phys. Rev. D34:2746(1986)

[100] Kajantie, K., Kataja, M., McLerran, L., Ruuskanen, P. V., Phys. Rev. D34:811(1986)

[101] Pisut, J., Acta Physica Polonica B17:911(1986); Csernai, V., Lichard, P., Pisut, J., Z. Phys. C31:163(1986)

[102] Kajantie, K., Proc. of Quark Matter '86, Nucl. Phys. A, to be published

[103] Pisarski, R., Phys. Lett. 110B:155(1982)

[104] Bochkarov A. I., Shaposhnikov, M., E., Nucl. Phys. B268:220(1986)

[105] *Siemens P., Chiu, S., A., Phys. Rev. Lett. 55:1266(1986)*

[106] *Matsui T., Satz, H., BNL Preprint BNL-38344 1986*

[107] *Biro, T., Barz, H., Lukacs B., Zimanyi, J., Nucl. Phys. A386:617(1982)*

[108] *Müller B., Rafelski, J., Phys. Rev. Lett. 48:1066(1982)*

[109] *Redlich, K., Z. Phys. C27:633(1985)*

[110] *Glendenning N., Rafelski, J., Phys. Rev. C31:823(1985)*

[111] *Kapusta J., Mekjian, A., Phys. Rev. D33:1304(1986)*

[112] *Matsui, T., McLerran, L., Svetitsky, B., Phys. Rev. D34:783(1986); MIT preprint MIT-CTP-1344 (1986).*

[113] *Kajantie, K., Kataja, M., Ruuskanen, P. V., Phys. Lett. 179B:153(1986)*

[114] *Rafelski J., Müller, B., GSI Preprint GSI-86-7 (1986).*

[115] *McLerran, L., Proceedings of Quark-Matter 86, Asilomar, Ca. (1986).*

[116] *Koch, P., Müller, B., Rafelski, J., Physics Reports 142:167(1986)*

[117] *Gyulassy, M., Kauffmann, S., Wilson, L. W., Phys. Rev.C 20:2267(1979)*

[118] *Pratt, S., Phys. Rev. Lett. 53:1219(1984); Phys. Rev. D33:72(1986) ; Phys. Rev. D33:1314(1986)*

[119] *W. A. Zajc, Proceedings of RHIC Workshop, BNL-51921.*

Figure Captions

1. For lattice computations to be valid, the points have to lie on the solid line (see text).

2. Energy density scaled by T^4 as a function of T. The arrow gives the level of the leading perturbative result.

3. A collision of two large nuclei A + B in a space-time diagram.

4. E/S vs ϵ in the MIT bag model.

5. p_T vs multiplicity in head on heavy ion collisions for an ideal gas equation of state (upper curve) and a bag model (lower curve).

6. p_T vs dN/dy scaled by 1/A for a variety of A.

7. Average p_T vs dN/dy for a variety of particles.

8. p_T distributions for a variety of particles.

9. An attempt to fit the JACEE cosmic ray data with a bag model and ideal gas equation of state. The upper curve is the ideal gas.

10. Flow distributions as measured by Gustafsson et. al.

11. Mass distribution of dileptons at $y \approx 0$ from two flows with the same dN_π/dy but different T_i.

12. The transverse mass distribution of dileptons with $M = 0.8$ GeV $\approx m_\rho$ for a 1 + 3 d flow with parameters as marked on the figure. The dashed line shows the result for a 1 + 1 d flow with no transverse flow.

13. The paths which two particles may take to coincidence detectors.

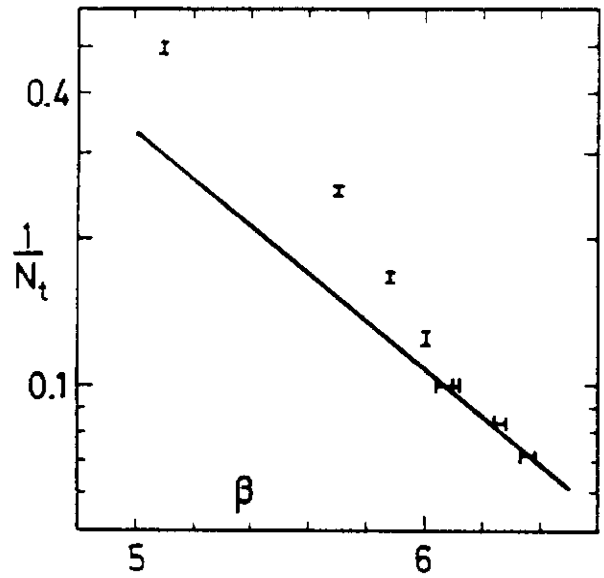

0.4
0.1
$\frac{1}{N_t}$
β
5
6

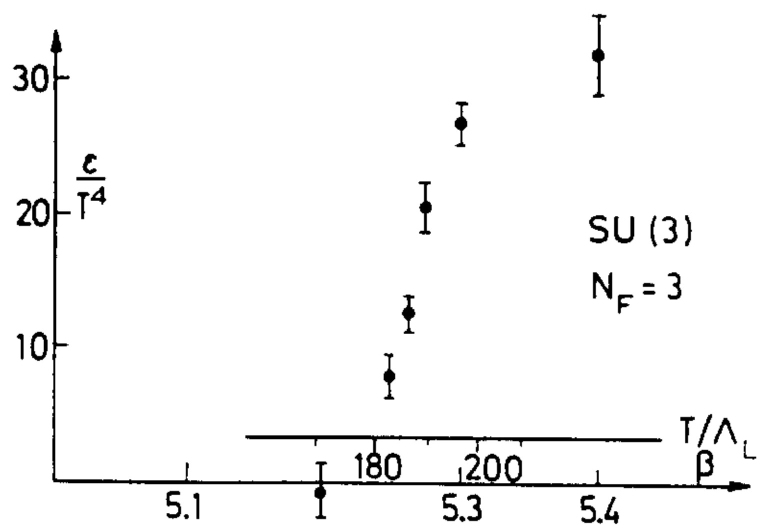

30
20
10
$\frac{\epsilon}{T^4}$
SU (3)
$N_F = 3$
T/Λ_L
180
200
β
5.1
5.3
5.4

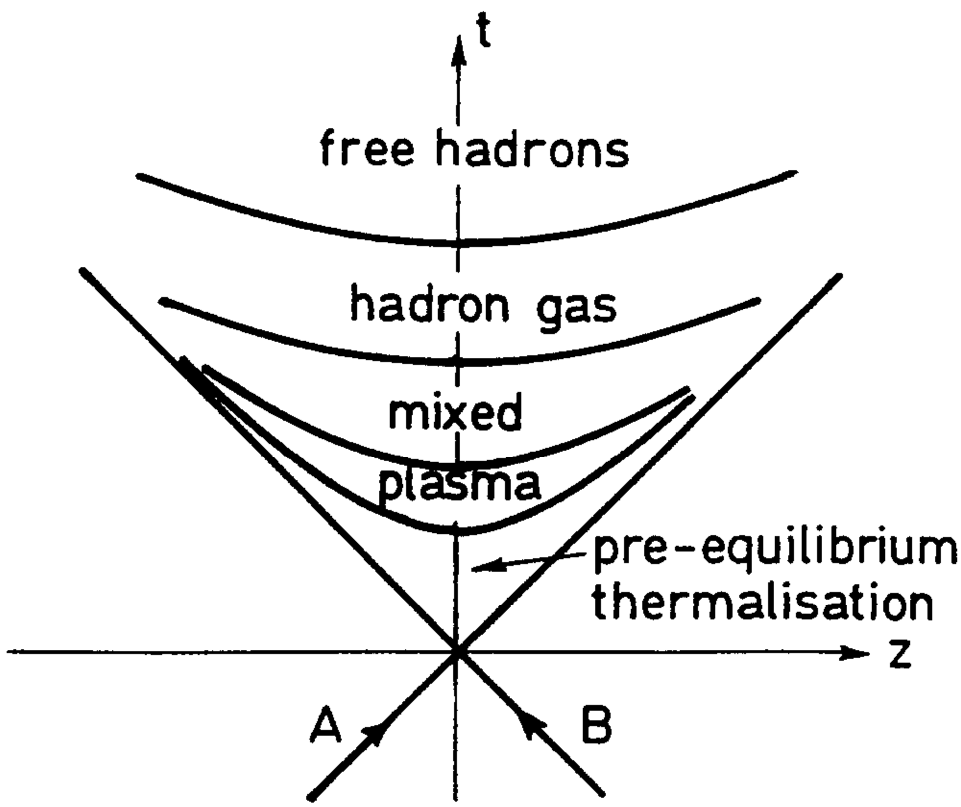
t
free hadrons
hadron gas
mixed
plasma
pre-equilibrium
thermalisation
z
A
B

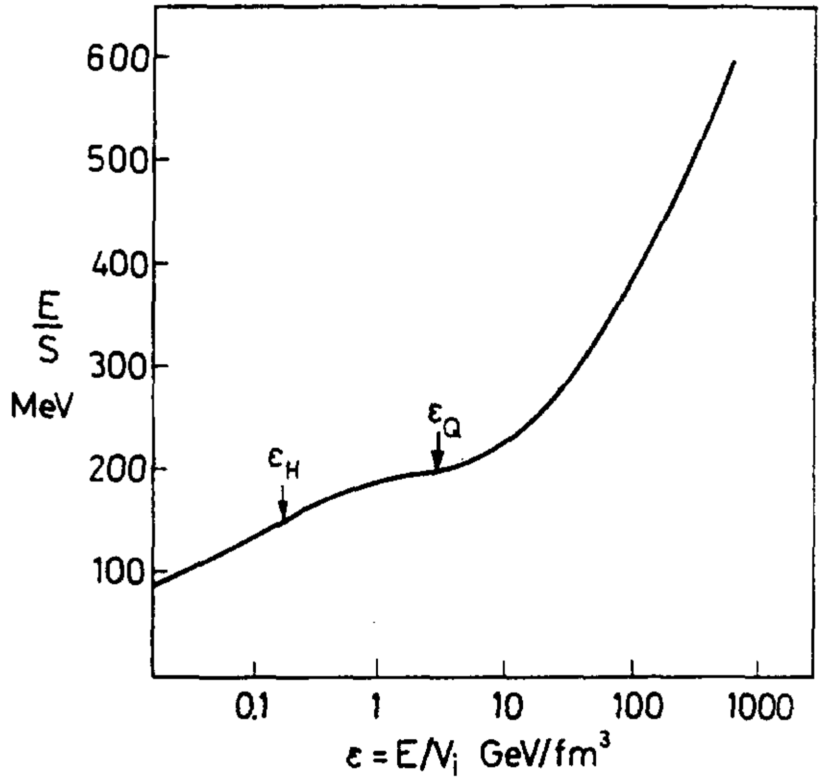
600
500
400
300
200
100
E/S
MeV
ε_H
ε_Q
0.1
1
10
100
1000
ε = E/V_i GeV/fm³

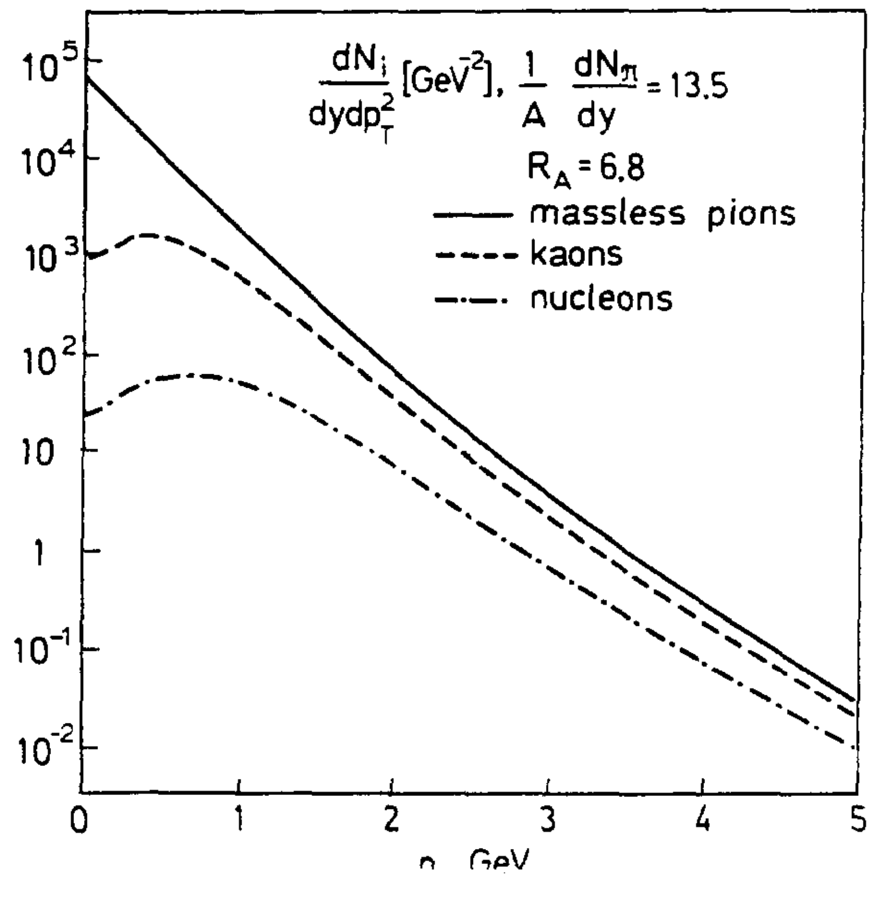
dN_i/dydp_T² [GeV⁻²], 1/A dN_π/dy = 13.5
R_A = 6.8
massless pions
kaons
nucleons
10⁵
10⁴
10³
10²
10
1
10⁻¹
10⁻²
0
1
2
3
4
5

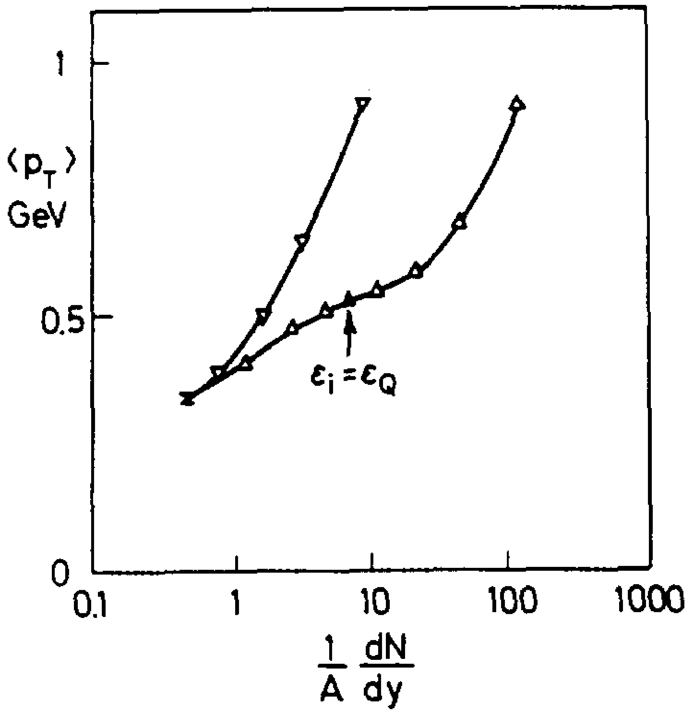

⟨p_T⟩ GeV
1
0.5
0
0.1
1
10
100
1000
ε_i = ε_Q
1/A dN/dy

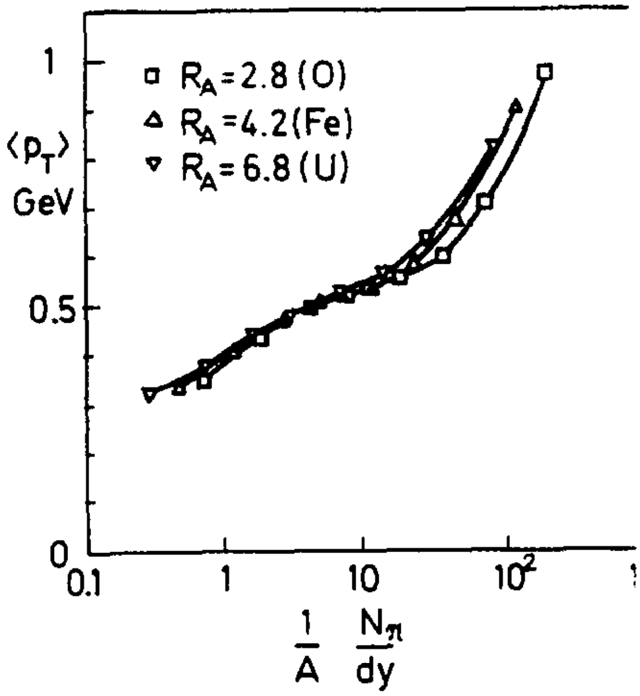

R_A = 2.8 (O)
R_A = 4.2 (Fe)
R_A = 6.8 (U)
⟨p_T⟩ GeV
1
0.5
0
0.1
1
10
10^2
1/A N_π/dy

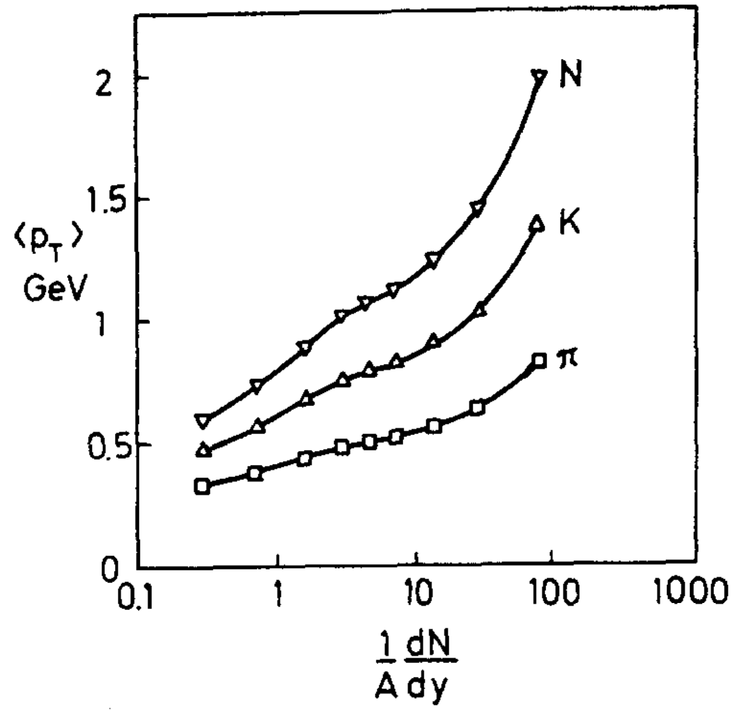

⟨p_T⟩ GeV
2
1.5
1
0.5
0
0.1
1
10
100
1000
N
K
π
1/A dN/dy

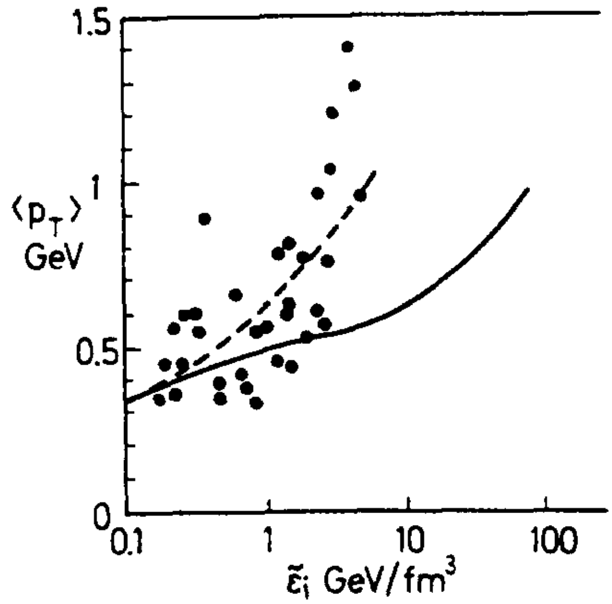

⟨p_T⟩ GeV
1.5
1
0.5
0
0.1
1
10
100
ε̃_i GeV/fm^3

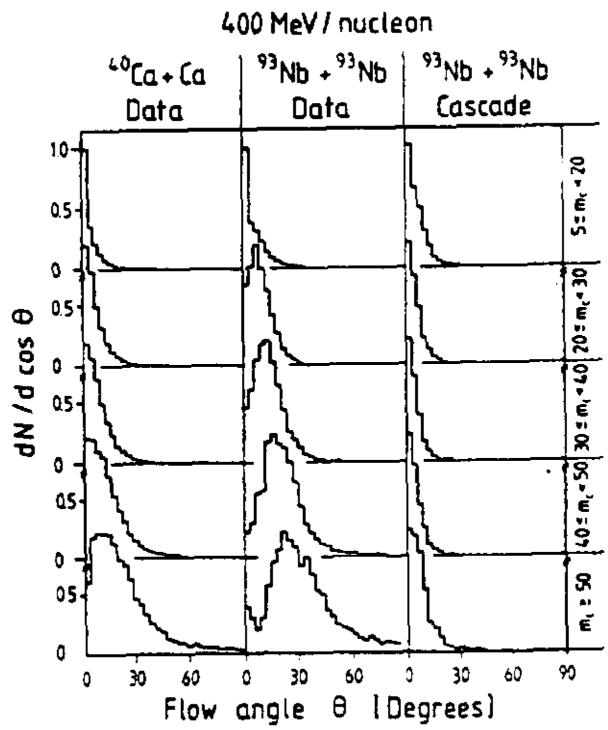
400 MeV / nucleon
^{40}Ca + Ca
Data
^{93}Nb + ^{93}Nb
Data
^{93}Nb + ^{93}Nb
Cascade
dN / d cos θ
1.0
0.5
0
5 ≤ m$_c$ < 20
20 ≤ m$_c$ < 30
30 ≤ m$_c$ < 40
40 ≤ m$_c$ < 50
m$_c$ ≥ 50
0
30
60
90
Flow angle θ [Degrees]

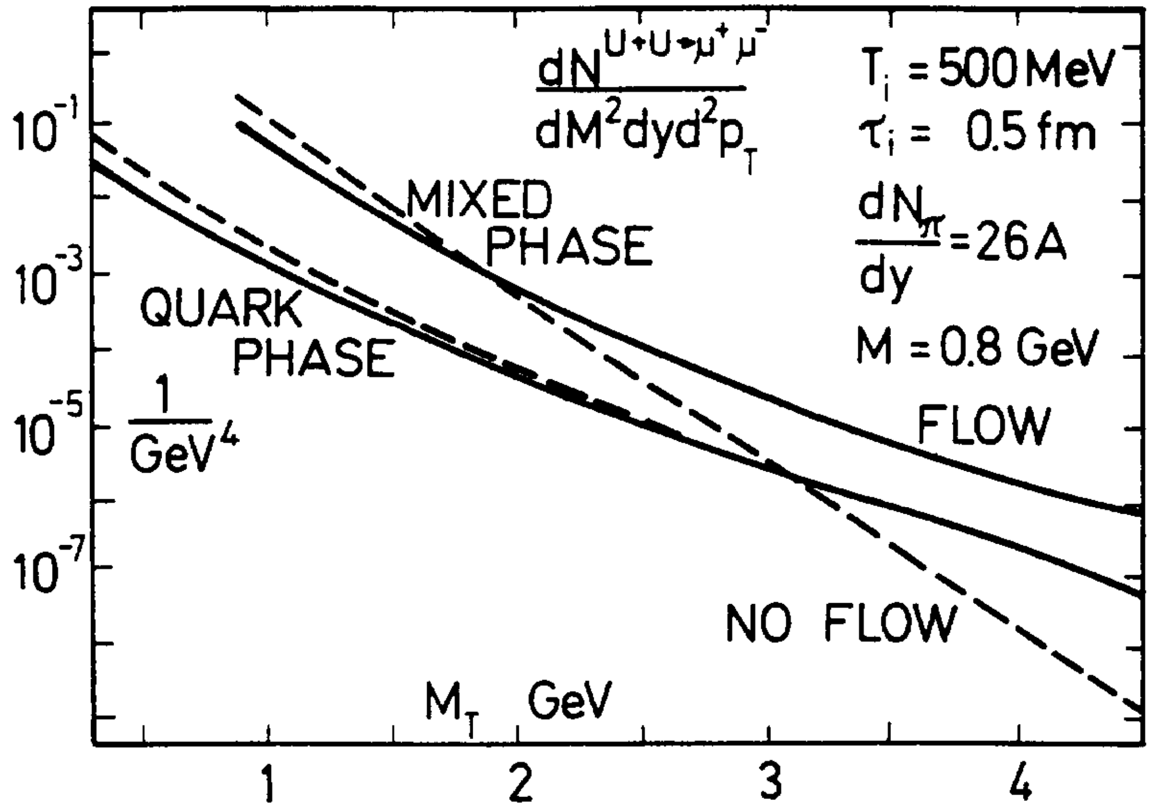

$\frac{dN^{U+U\to\mu^+\mu^-}}{dM^2 dy d^2p_T}$
T_i = 500 MeV
τ_i = 0.5 fm
$\frac{dN_\pi}{dy}$ = 26 A
M = 0.8 GeV
MIXED PHASE
QUARK PHASE
FLOW
NO FLOW
$\frac{1}{GeV^4}$
10^{-1}
10^{-3}
10^{-5}
10^{-7}
M_T GeV
1
2
3
4

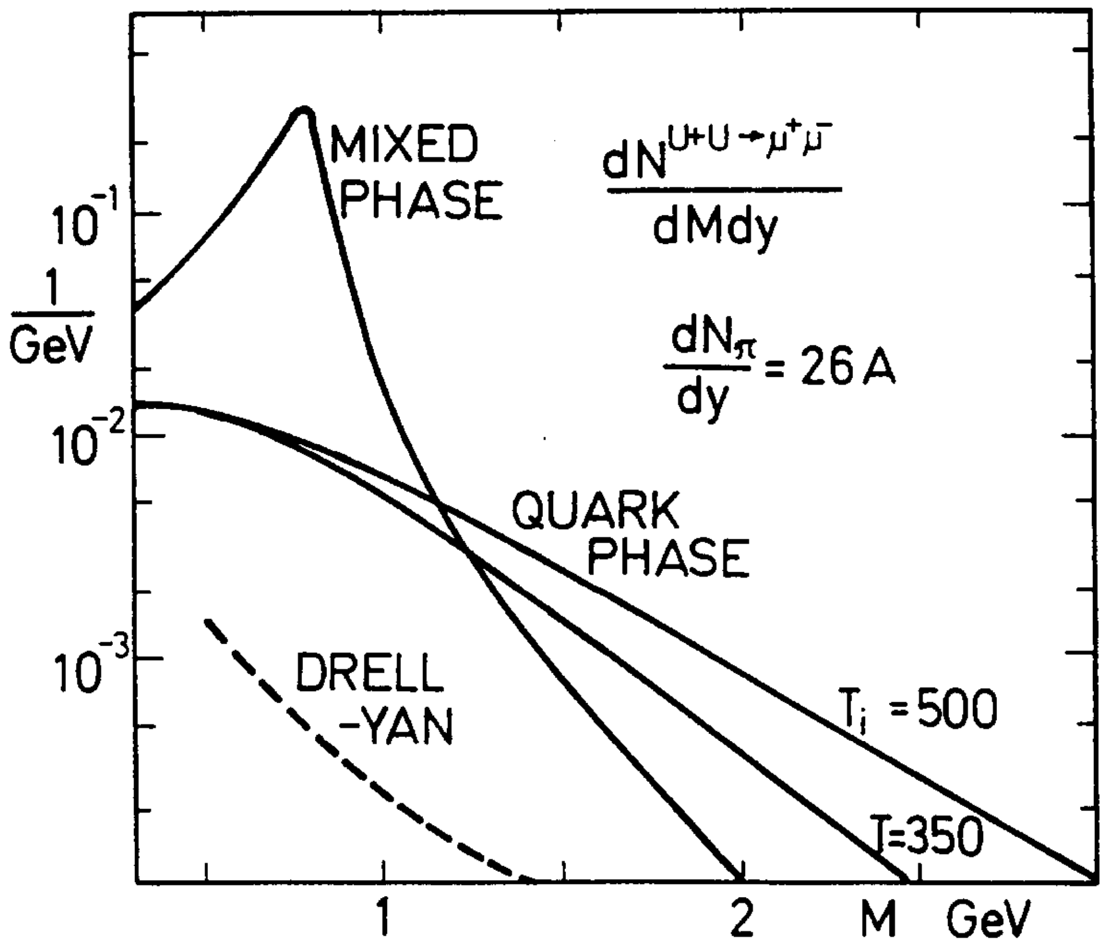

MIXED PHASE
$\frac{dN^{U+U\to\mu^+\mu^-}}{dMdy}$
$\frac{1}{GeV}$
$\frac{dN_\pi}{dy}$ = 26 A
10^{-1}
10^{-2}
10^{-3}
QUARK PHASE
DRELL -YAN
T_i = 500
T=350
1
2
M GeV